

**STM-induced photon emission at the solid-liquid interface**

Karen Perronet and Fabrice Charra\*

CEA-Saclay, DSM-DRECAM-SPCSI, F-91191 Gif-sur-Yvette Cedex, France

(Received 5 September 2002; revised 18 December 2002; published 15 April 2003)

We extended scanning-tunneling-microscope- (STM-) induced photon emission from the metal surface to the solid-liquid interface. A Au(111)-Au junction immersed in a liquid droplet was studied. We observed the same voltage threshold for photon emission when adding liquid compared to the air medium, a strong decrease of the apparent tunnel barrier height, and redshifted emission spectra, except in the case of an IR-absorptive liquid. This is attributed to the refractive index of the liquid. This technique could be applied, e.g., to the study of STM-induced photon emission of self-assembled molecule monolayers formed on a Au(111) substrate.

DOI: 10.1103/PhysRevB.67.153402

PACS number(s): 73.20.Mf, 73.40.Gk, 78.68.+m

**I. INTRODUCTION**

The technique of light emission induced by a scanning tunneling microscope (STM) has been greatly improved in the last ten years and has become a new information source for surfaces of metals and semiconductors.<sup>1</sup> In particular atomic resolution has been obtained both on the photon emission map and on the topography of a gold (110) substrate,<sup>2</sup> chemical information can be deduced from light spectra taken during the scan,<sup>3</sup> and both the topography and photon map of molecules deposited on a Cu surface under ultrahigh vacuum (UHV) have been observed with molecular resolution.<sup>4</sup>

In addition, numerous studies of self-assembled monolayers of molecules at the solid-liquid interface have been achieved with the STM (Ref. 5) or electrochemical STM (Ref. 6). However, the light emission of a tunnel junction immersed in a solvent droplet has never been investigated. Only very preliminary results have been reported by Nishitani and Kasuya.<sup>7</sup>

In this paper, we report investigations of the STM-induced photon emission of a Au(111)/Au junction immersed in a liquid. Oppositely to Nishitani and Kasuya, we succeeded in detecting light emission at smooth conditions, i.e., with moderate biases and tunnel currents. This enables the measurement of the voltage emission threshold, the apparent height of the tunnel barrier, and the spectra of the emitted light for all liquids. We compare our results with those obtained at air in the same setup or under UHV and conclude on the influence of the dielectric constant  $\epsilon(\omega=0)$  and of the refractive index of the liquids.

**II. METHOD**

A Au(111)/Au junction immersed in a liquid droplet was studied with a homemade STM. Liquids were chosen to be hydrophobic to avoid problems due to contamination with water and with a good electrochemical stability to achieve spectroscopic measurements. Gold samples were prepared by evaporating pure gold onto freshly cleaved mica. Tips were made from 250  $\mu\text{m}$  gold wires and mechanically cut. Four liquids were considered: phenyloctane, dodecan-4-ol, tetradecane, and perfluorooctane (cf. Table I). Phenyloctane and tetradecane were chosen because they are very commonly

used in STM structural studies of self-assembled monolayers, perfluorooctane has an unusually low refractive index and an increased transparency in the infrared (IR), and dodecanol has a higher dielectric constant at  $\omega=0$ . We also tried to work with dimethyl sulfoxide whose dielectric constant is quite high and which was tested by Nishitani but this liquid is slightly electrically conductive and the study with the STM was impossible to achieve.

**A. Excitation spectroscopy**

The light emitted at the tunnel junction was collected by a large-aperture lens and focused onto a single-photon counting module (EGG, SPCM-AQ-15, with 60 cps dark count). The spectral range of detection was 400–1060 nm. Tunnel current characteristics  $I(V)$  and photon counting rates  $N(V)$ , as well as  $I(s)$  and  $N(s)$  ( $s$  being the tip height), were recorded on different points of the sample. A typical set of measurements corresponds to 128 points taken in  $\approx 1.5$  s, that is to say, for  $I(s)$  curves, a rate of  $\approx 5$   $\text{\AA}/\text{s}$  for tip retraction. Thus, we avoid experimental artifacts mentioned in Ref. 9.

**B. Emission spectroscopy**

We measured the wavelength distribution of the light emitted by the tunnel junction immersed in air, perfluorooctane, and tetradecane. In this case, the light was collected by a microscope objective, then passed through a dispersing prism (flint glass), and finally focused on a CCD array (Andor, DU401-BR-DD) cooled at  $-70^\circ\text{C}$ . The spectral range of detection is 400–1150 nm. The spectral resolution is about 30 nm in the infrared and 5 nm at 600 nm, according for the dispersive power of the prism and to the ability to focus the light on the camera (in the nondispersive direction, the size of the image did not exceed 4 pixels in air and 6 in liquids). The light source being smaller than the wavelength, an entrance slit is not necessary in this setup. Thus we avoid losses associated with intermediate images. Furthermore, the lower dispersive power of the prism in the infrared allows an increased sensitivity in this spectral range.

**III. EXPERIMENTAL RESULTS****A. Voltage spectroscopy**

Figure 1 shows a typical set of characteristics of the studied junctions. The general shapes of the curves are similar to

TABLE I. Characteristics of studied solvents and experimental results.

Medium	Dielectric constant ( $\omega=0$ ) <sup>a</sup>	Refractive index <sup>a, b</sup>	Emission threshold (V)	Apparent barrier height (eV)
Phenyl octane	2.26	1.49	between 1.2V and 1.3V	0.6
Perfluorooctane	1.76 <sup>c</sup>	1.28		0.3
Tetradecane	2.03	1.43		1.1
Dodecan-4-ol	$\approx 4$ <sup>d</sup>	1.44 <sup>e</sup>		1.3
UHV	1	1		3.0

<sup>a</sup>References 8.<sup>b</sup>For Na D rays.<sup>c</sup>Value reported for perfluorohexane.<sup>d</sup>Estimation according to the decanol series figuring in the Handbook (Ref. 8).<sup>e</sup>Value reported for dodecan-1-ol.

those obtained in air or under vacuum. The  $I(V)$  relationship is linear between  $-1$  and  $1$  V and nonlinear above.  $N(V)$  curves are symmetrical, at the dark noise level for low tunnel biases and increasing above a threshold bias. In air, the threshold value is between 1.2 and 1.3 V. For all other studied liquids, we also recorded a signal for biases starting above 1.2 V. As is known, the mechanism of excitation of the plasmon modes involves inelastic tunnelling,<sup>10</sup> so that the energy of the emitted photons is less or equal to  $eV_{tunnel}$  where  $V_{tunnel}$  is the tip-sample bias. Due to the limited spectral range of the detector, we are not able to detect photons with a wavelength larger than 1060 nm, i.e., with an energy less than 1.2 eV. Hence, the observed emission threshold corresponds to the detector's cutoff frequency.

### B. Tip height spectroscopy

We recorded variations of current and photon emission versus tip retraction [ $I(s)$  and  $N(s)$ ] starting from two different scan conditions. At  $V_{sample}=2$  V,  $I=2$  nA, we ob-

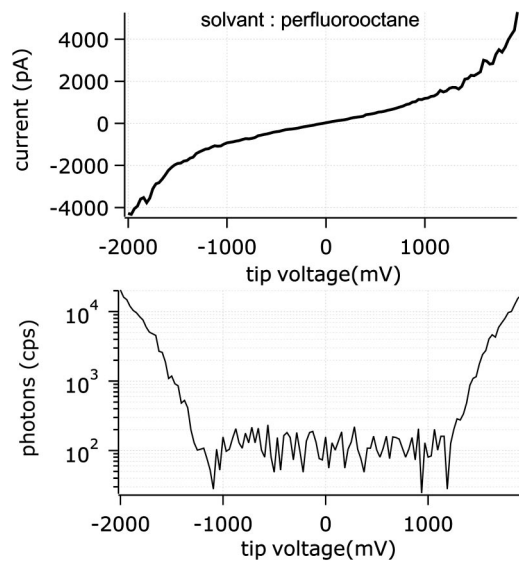


FIG. 1. Voltage spectroscopy for a Au(111)/Au junction in perfluorooctane.

serve an exponential decay of  $I(s)$  and  $N(s)$  in air, in UHV, and in all liquids. But with  $V_{sample}=1.6$  V,  $I=5$  nA (i.e., starting the measurement closer to the sample), the behavior of the natural logarithm of both current and photon emission is no longer linear (cf. Fig. 2). We can see two different domains with two distinct decay constants, the one measured close to the sample being smaller both in UHV and in liquid. Furthermore, in each case, photon emission is parallel to the current in the whole interval of  $s$ .<sup>11</sup>

We can deduce the apparent height of the tunnel barrier<sup>12</sup> using the formula

$$\Phi_{ap}(eV) = 0.952 \left[ \frac{d \ln I}{ds(\text{\AA})} \right]^2. \quad (1)$$

The values are reported in Table I and correspond to the barrier measured for larger  $s$ . They are lower in liquids than in UHV.

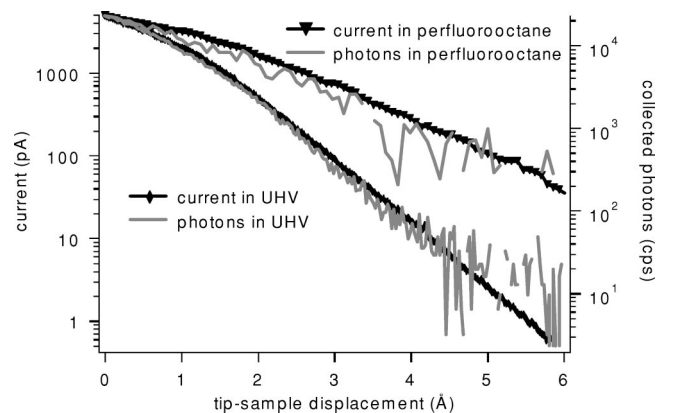


FIG. 2. Tip height spectroscopy obtained for perfluorooctane and UHV. Scan conditions are 5 nA,  $V_{sample}=1.6$  V. Current (in pA) and photon emission (in counts per second) are plotted vs. tip retraction. The Y axis is in logarithmic scale for all curves. Photon emission in perfluorooctane data have been multiplied by 20 for easier comparison. Notice the existence of two domains with different barrier characteristics.

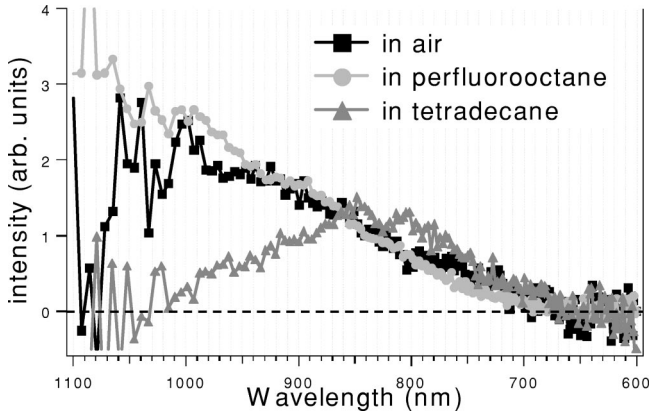


FIG. 3. Emission spectra in air, perfluorooctane, and tetradecane. All spectra are recorded at  $V_{sample} = 1.8$  V,  $I = 2$  nA with a Pt/Ir tip, and corrected for the instrumental response.

### C. Emission spectroscopy

In Fig. 3 are reported the spectra of the light emitted for tetradecane, perfluorooctane, and air, all recorded with  $V_{sample} = 1.8$  V,  $I = 2$  nA and with a Pt/Ir tip. We recorded also with gold tips, but their shape is less stable than those of Pt/Ir tips under these scan conditions and spectra were less reproducible.

All the spectra plotted in Fig. 3 are corrected for the non-linear dispersion of the prism and for the quantum efficiency of the detector. They have the same shape as the spectra recorded on Ti by Berndt *et al.*<sup>13</sup> which were also corrected for instrumental response: except for tetradecane which exhibits a clear peak at 900 nm, the spectra are more intense in the IR, but because of the limited spectral range of the detector, we cannot locate any maximum. The spectrum in perfluorooctane is slightly redshifted, compared to the one in air.

## IV. DISCUSSION

Electron tunneling through organic molecules or liquid water has been studied recently in several experimental<sup>14,15</sup> and theoretical<sup>16,17</sup> papers. The effective decay constants ( $\approx 1 \text{ \AA}^{-1}$ ) measured for tetradecane and dodecane-4-ol are quantitatively fully consistent with a one-step tunneling from tip to sample through the liquid.<sup>14</sup> The lowering of the barrier height, compared with vacuum, is due to the dielectric constant at  $\omega = \Phi_{ap}/\hbar$  of the liquid and to the opening of reduced-potential pathways (virtual localized intermediate states) through molecules.<sup>16</sup> This effect is even increased for phenyloctane, as expected for a molecule with a conjugated moiety, and for perfluorooctane, maybe because of the partial charging of the carbon backbone. The direct tunneling mechanism is confirmed by the observation of bias thresholds for light emission corresponding exactly to the low-energy limit of detector sensitivity and an onset of the photon emission spectra corresponding systematically to the applied biases ( $\lambda_{cutoff} = hc/eV_{tunnel}$ ). As a matter of fact, in this situation, the energy gained by the electron transferred from tip to sample is fully transmitted to the photon, which confirms that the whole electron transfer corresponds to a single-quantum process.

TABLE II. Estimation of the first plasmon mode energy.

Medium	Refractive index	Plasmon mode energy (eV)
Vacuum	1	1.4
Perfluorooctane	1.28	1.1
Tetradecane	1.43	1
Dodecanol	1.44	1
Phenyloctane	1.49	1

These results contradict the conclusion of Nishitani and Kasuya.<sup>7</sup> Despite higher  $\epsilon(\omega=0)$  in liquids, the applied voltage is totally transmitted to the photon. More specifically, an intermediate mechanism involving electrons of the solvent molecules in the coupling with the plasmon mode may exist but is not dominating.

Furthermore, we noticed that even with a liquid,  $I(s)$  and  $N(s)$  curves have the same decay behavior and this holds for all the emission spectra. This shows that the basic mechanism of photon emission is not changed when increasing the tunneling path length in the liquid.

The dielectric constant at  $\omega$  modifies, however, the plasmon mode frequency. We can quantify this modification using the so-called sphere-above-plane geometry<sup>18</sup> to model the junction. When the tunnel contact is established, we can assume  $d \ll R \ll \lambda$  ( $d$  being the tip-sample distance,  $R$  the curvature radius of the tip, and  $\lambda$  the mean wavelength of the plasmon mode). In our case, tip, and sample are made of the same metal. It has been shown that the localized plasmon modes exist for<sup>18,19</sup>

$$\text{Re}\left(\frac{\epsilon_{\text{solvent}}(\omega)}{\epsilon(\omega)}\right) = -(l+1/2) \sqrt{\frac{d}{2R}}. \quad (2)$$

At the frequencies considered, the Drude model is correct to describe the metal and then  $\epsilon(\omega) = \omega_p^2/\omega^2$  where  $\omega_p$  is the plasma pulsation of the metal. So the plasmon pulsations are given by

$$\omega^2 = \sqrt{\frac{d}{2R}}(l+1/2) \frac{\omega_p^2}{\epsilon_{\text{solvent}}(\omega)}. \quad (3)$$

As a consequence, the higher the refractive index, the more the emission spectrum is redshifted and the less the detector is sensitive. We can estimate the first plasmon mode energy (for  $l=0$ ). Using  $d \approx 1$  nm and  $R \approx 100$  nm (typical values for a gold tip) we get, from Eq. (2),  $\epsilon(\omega) \approx -30\epsilon_{\text{solvent}}(\omega)$ . The calculated values, using for  $\epsilon(\omega)$  the values given in Ref. 8, are reported in Table II. They are consistent with the redshifted spectrum observed in perfluorooctane but not with the blueshift in tetradecane. However, it is known that there is a peak at 1100 nm in the infrared absorption spectrum of tetradecane corresponding to the second overtone of the CH bond band (nonzero  $\text{Im}[\epsilon(\omega)]$ ). This absorption can be responsible for an overdamped tip-induced plasmon mode in the infrared for tetradecane and so for the apparent blueshift observed. On the contrary, perfluorooctane has no CH bond, and consequently its spectrum is redshifted as expected.

Finally, if the refractive index increases, the difference between the plasmon modes of successive indices decreases. So more modes are available for excitations by the tunneling electron, and consequently, the probability to excite the first (dipolarlike) mode, i.e., the one with the more efficient radiative coupling, decreases.

### V. CONCLUSION

We have investigated the conditions of STM-induced light emission at the solid-liquid interface for several liquids and the characteristics of the tunnel barrier in these conditions. We have shown that the apparent height of the tunnel barrier is reduced, because the solvent-electron presence gives to the tunneling electron more pathways to go through the barrier.

The presence of the liquid does not modify the main mechanism of light emission, i.e., the coupling between the inelastic tunnel electrons and the localized plasmon modes.

We have shown that the real part of the dielectric constant at  $\omega$  of the liquid is responsible for a redshift of the light emitted, and its imaginary part sometimes give rises to an absorption in the IR. For high refractive index solvents, the spectral range of the emitted light can be outside the spectral window of usual detectors and the emission efficiency may also decrease because more plasmon modes (and in particular the nonradiative ones) can be excited.

These observations open new opportunities such as the investigation of the influence on STM-induced photon emission of a self-assembled molecule monolayer formed on a Au(111) substrate.

---

\*Electronic address: fabrice.charra@cea.fr

- <sup>1</sup>R. Berndt, in *Scanning Probe Microscopy*, edited by R. Wiesendanger, Springer Series Nanoscience and Technology (Springer-Verlag, Berlin, 2000), p. 97.
- <sup>2</sup>R. Berndt, R. Gaisch, W.D. Schneider, J.K. Gimzewski, B. Reihl, R.R. Schlittler, and M. Tschudy, *Phys. Rev. Lett.* **74**, 102 (1995).
- <sup>3</sup>A. Downes, P. Guaino, and P. Dumas, *Appl. Phys. Lett.* **80**, 380 (2002).
- <sup>4</sup>G. Hoffmann, L. Libioulle, and R. Berndt, *Phys. Rev. B* **65**, 212107 (2002).
- <sup>5</sup>F. Charra and J. Cousty, *Phys. Rev. Lett.* **80**, 1682 (1998).
- <sup>6</sup>See, e.g., N.J. Tao, C.Z. Li, and H.X. He, *J. Electroanal. Chem.* **492**, 81 (2000).
- <sup>7</sup>R. Nishitani and A. Kasuya, *Surf. Sci.* **433-435**, 283 (1999).
- <sup>8</sup>*Handbook of Chemistry and Physics*, 80th ed., edited by David R. Lide (CRC Press, Boca Raton, FL, 2000).
- <sup>9</sup>L. Olesen, M. Brandbyge, M.R. Sørensen, K.W. Jacobsen, E. Lægsgaard, I. Stensgaard, and F. Besenbacher, *Phys. Rev. Lett.* **76**, 1485 (1996).
- <sup>10</sup>B.N.J. Persson and A. Baratoff, *Phys. Rev. Lett.* **68**, 3224 (1992).
- <sup>11</sup>R. Berndt, J.K. Gimzewski, and P. Johansson, *Phys. Rev. Lett.* **71**, 3493 (1993).
- <sup>12</sup>N.D. Lang, *Phys. Rev. B* **37**, 10 395 (1988).
- <sup>13</sup>R. Berndt, J.K. Gimzewski, and R.R. Schlittler, *Ultramicroscopy* **42-44**, 355 (1992).
- <sup>14</sup>D.E. Khoshtariya, T.D. Dolidze, L.D. Zusman, and D.H. Waldeck, *J. Phys. Chem. A* **105**, 1818 (2001).
- <sup>15</sup>G. Nagy, D. Mayer, and Th. Wandlowski, *Phys. Chem. Commun.* **5**, 112 (2002).
- <sup>16</sup>W. Schmickler, *Surf. Sci.* **335**, 416 (1995).
- <sup>17</sup>U. Peskin, Å. Edlund, I. Bar-On, M. Galperin, and A. Nitzan, *J. Chem. Phys.* **111**, 7558 (1999).
- <sup>18</sup>A. Mal'Shukov, *Phys. Rep.* **194**, 343 (1990).
- <sup>19</sup>R.W. Rendell, D.J. Scalapino, and B. Mühlshlegel, *Phys. Rev. Lett.* **41**, 1746 (1978).